Asian Journal of Fuzzy and Applied Mathematics (ISSN: 2321 – 564X)
Volume 03 – Issue 01, January 2015

Transient Analyses of Grounding Systems Subjected by Lightning Surge Currents through Fuzzy-Based Models of Input Impedance in the Frequency Domain

Zahra Samiee[1], Saeed Reza Ostadzadeh[2*]

[1] Arak University
Arak, Iran

[2] Arak University
Arak, Iran
[*]*Corresponding author's email: s-ostadzadeh [AT] araku.ac.ir*

ABSTRACT— ***In this paper, fuzzy-based models which is special for electromagnetic problems are applied to model the input impedance of the grounding systems such as vertical and horizontal electrodes. In each model, the behavior of the electrode is first extracted by if-then rules, and then the effects of different parameters for instance soil resistivity and electrode radius are separately extracted as simple curves. Then using spatial membership functions, these effects are combined so as to create simultaneous effects of all parameters on the input impedance. As a result, the input impedance is efficiently predicted for arbitrary resistivity of soil, radius, and normalized length of electrodes. Finally through fast Fourier transform (FFT) and inverse fast Fourier transform (IFFT), the transient voltage for each electrode is efficiently computed.***

Keywords— Grounding system, Fuzzy inference, input impedance.

---

1. INTRODUCTION

Grounding systems such as vertical and horizontal electrodes are often used in power systems to discharge lightning current into earth without any damage to people and installations [1-6]. Figure 1 shows schematic diagram of such grounding systems under lightning stroke.

Transient voltage of grounding system (defined electrical potential of the grounding electrodes with respect to a reference point at infinite) is of great practical importance, because firstly it is able to reveal the maximum voltage level that is submitted to the ground, secondly it is evaluates the time that the ground is subjected to certain levels of transient voltage. Safety criteria are based upon minimizing this parameter. It is usually computed as following:

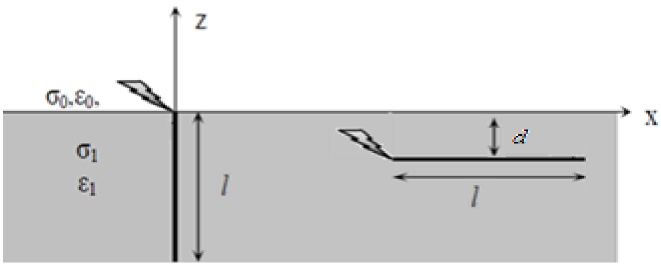

Figure 1: Schematic diagrams of conventional grounding systems.

$$v(t) = F^{-1}\{F(i(t))Z(jf)\} \tag{1}$$

Where F and F^{-1} denote Fourier and inverse Fourier transformations respectively, and $Z(jf)$ is input impedance of the grounding system in the frequency domain, and defined as following:

$$Z(jf) = \frac{V(jf)}{I(jf)} \tag{2}$$

where $V(jf)$ and $I(jf)$ are electrical potential and electrical current in the frequency domain respectively. There are two different current wave forms, $i(t)$, corresponding to first and subsequent return strokes [4], as following:

$$i(t) = \frac{I_0}{\eta} \frac{(t/\tau_1)^n}{1+(t/\tau_1)^n} \exp(-t/\tau_2) \tag{3}$$

and

$$\eta = \exp\left[-(\tau_1/\tau_2)(n\tau_2/\tau_1))^{1/n}\right] \tag{4}$$

Where I_0 is the amplitude of current, τ_1 is the front time constant, τ_2 is decay time constant, n is an exponent having value between 2 to 10, and η is the amplitude of the correction factor. These parameters are given in the table 1.

Table 1. Heidler parameters for lightning current of first and subsequent stroke.

Parameters	I_{01} (KA)	τ_{11} (μs)	τ_{12} (μs)	n_1	I_{02} (KA)	τ_{21} (μs)	τ_{22} (μs)	n_2
First Stroke	28	1.8	92	2	---	---	---	---
Subsequent stroke	10.7	0.25	2.5	2	6.5	2.1	230	2

To the best our knowledge, there is no closed form solution for input impedance except RLC and TLM [1] which are based on quasi static approximation and valid when the length of electrode is less than one-tenth of the wave length in the earth. Therefore proposing comprehensive model is vital.

Tayarani et al in 2001 an intelligent model [7] based upon fuzzy inference for electromagnetic problems proposed, and since then has been found several applications for example in analyzing nonlinearly loaded antenna array [8, 9]. In this method of fuzzy abbreviated to MoF from now on, behavior of the problem is represented as circular movement in polar plane, and then effects of problem parameters are extracted as displacement and compressing or spreading this movement. Further information about the MoF is given in the next section.

This paper is organized as follows. In section II, fuzzy behavior of the vertical electrode is linguistically introduced, and in following, the effect of electrical parameters of soil and electrode radius on the input impedance is easily extracted using spatial membership functions [10]. In section III, The same as vertical electrode a fuzzy model is introduced for horizontal one. Finally in section IV, transient voltages of the grounding system for the first and subsequent lightning currents are efficiently computed.

2. BEHAVIOR OF VRTICAL ELECTELECTRODEE

In this section, consider a vertical electrode of length 10 m which is buried in the earth of electrical parameters $\varepsilon_r = 10$ and $\rho = 1000\Omega.m$.

To extract behavior of the vertical electrode, at first, the input impedance of the electrode in the frequency rage [1-10] MHz is computed by MoM. Figure 2(a) shows the amplitude versus phase of the input impedance in polar plane. In figure 2(a), as L/λ (L is electrode length) is increased, a circular movement is created. Inside this movement, three circles are distinguishable in such a way that these are converted to each other smoothly. To define these circles, three sets of starting points (stars, circles, and pluses in figure 2(b)) around $L/\lambda = 0.07, 0.17, 0.27$ are first chosen. These circles are shown in figure 2(b) as dashed circles whereas the input impedance is shown as solid curve.

Now, one can represent the circular movement through the fuzzy if-then rules as following:

$$\begin{cases} if \quad L/\lambda \quad belongs \quad to \quad small \quad set \rightarrow first \quad circle \\ if \quad L/\lambda \quad belongs \quad to \quad medium \quad set \rightarrow second \quad circle \\ if \quad L/\lambda \quad belongs \quad to \quad long \quad set \rightarrow third \quad circle \end{cases} \tag{4}$$

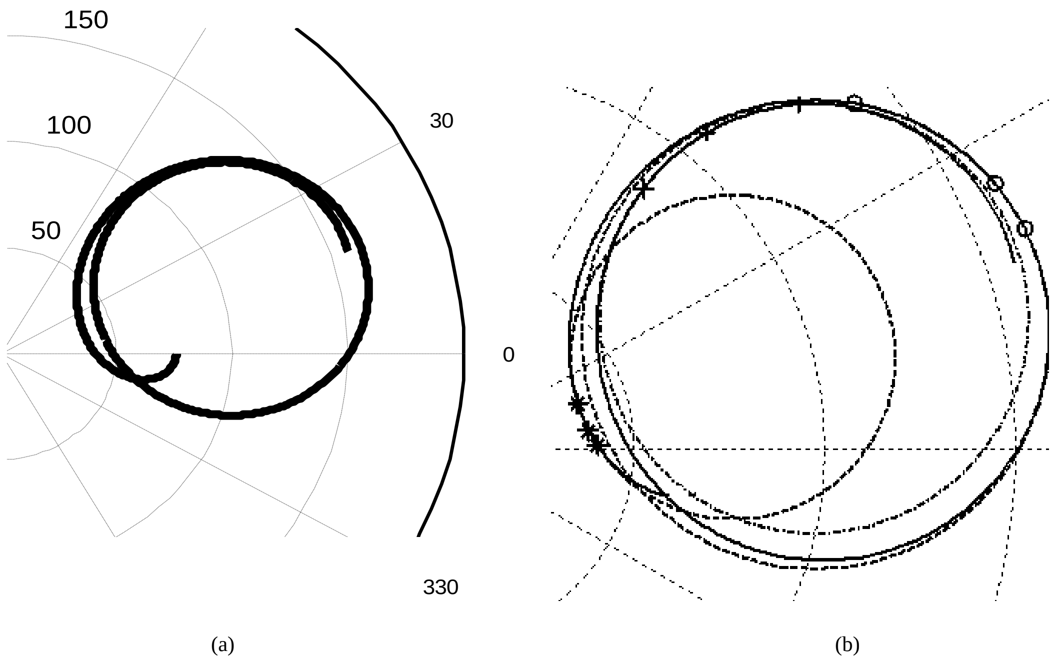

Figure 2: (a): Amplitude versus phase of input impedance (ohm) of vertical electrode. (b): figure (a) in addition to fitted circles.

Assigning membership function or belongingness for each fitted circle is the next step so that they have belongingness one on the fitted circles and smoothly decreasing to zero on the neighbor fitted circles. These functions are defined in [11].

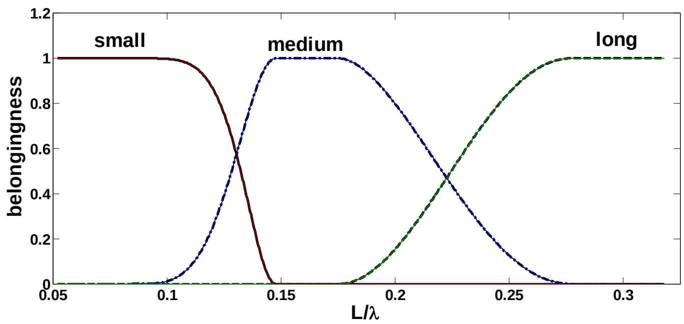

Figure 3: Membership functions for assigning three fotted circles.

Using Takagi-Sugeno method [7], the above rules is led to inferring one circle for each L/λ as follows:

$$\begin{cases} x(\frac{L}{\lambda}) = \sum_{i=1}^{3} x_i \alpha_i (\frac{L}{\lambda}) \\ y(\frac{L}{\lambda}) = \sum_{i=1}^{3} y_i \alpha_i (\frac{L}{\lambda}) \\ r(\frac{L}{\lambda}) = \sum_{i=1}^{3} r_i \alpha_i (\frac{L}{\lambda}) \end{cases} \tag{5}$$

in which $x_i, y_i, r_i, i = 1,2,3$ is center coordinates and radius of the fitted circles (dashed-dotted circles in figure 2(b)) and α_i's are membership functions in figure 3. Inferring one circle for each L/λ in this step is termed partial locus. A few fuzzy-inferred circles are shown in figure 4.

According to [7], to find the correct place of the input impedance on the each inferred circle, the partial phase (phase with respect to the centre of inferred circles) should be defined, and then modeled. The partial phase is shown in figure 5. Modeling partial phase is the same as partial locus except that circles are replaced with lines, that is

$$\begin{cases} if \quad L/\lambda \quad belongs \quad to \quad small \quad set \rightarrow first \quad line \\ if \quad L/\lambda \quad belongs \quad to \quad medium \quad set \rightarrow second \quad line \\ if \quad L/\lambda \quad belongs \quad to \quad long \quad set \rightarrow third \quad line \end{cases} \tag{6}$$

$$\begin{cases} m(\frac{L}{\lambda}) = \sum_{i=1}^{3} m_i \alpha_i'(\frac{L}{\lambda}) \\ n(\frac{L}{\lambda}) = \sum_{i=1}^{3} n_i \alpha_i'(\frac{L}{\lambda}) \end{cases} \tag{7}$$

in which $m_i, n_i, i = 1,2,3$ is slope and bias of the fitted lines (dashed lines in figure 5) ,α_i''s are membership functions in figure 5, and m, n are slope and bias for other values of L/λ.

Note that the markers (stars, pluses, and circles) in figure 5 are those used for modeling fitted circles.

Finally, the real and imaginary part of the induced voltage versus input value L/λ is computed through the below equation:

$$Z_{in}(L/\lambda) = x + jy + r\exp\{j(m \times L/\lambda + n)\} \tag{8}$$

in which, (x, y, r), and (m, n) are computed from equations (5) and (7) respectively, and $j = \sqrt{-1}$.

The membership functions in figures 3 and 5 from now on are considered as behavior of the grounded vertical electrode.

Figure 7 shows the predicted input impedance versus L/λ by the MoF, and MoM. As it is seen, excellent agreement is achieved.

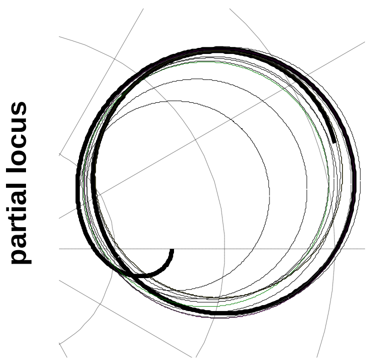

Figure 4: Fuzzy-inferred circles.

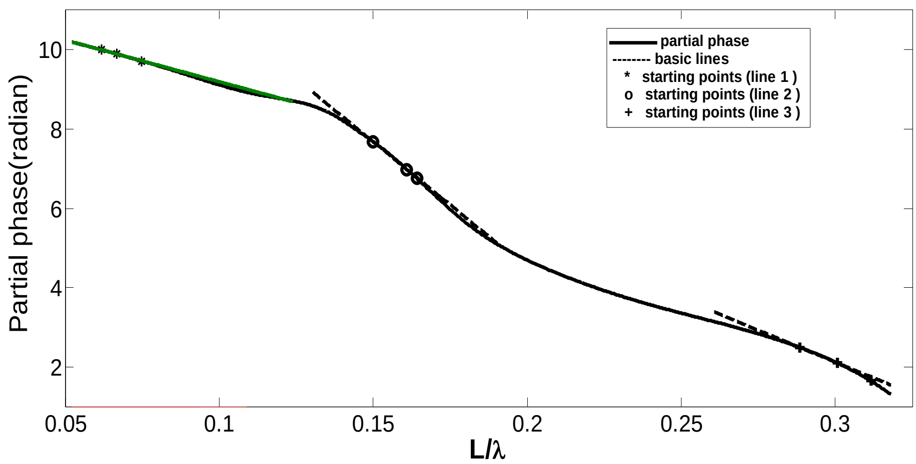

Figure 5: Partial phase as well as fitted lines.

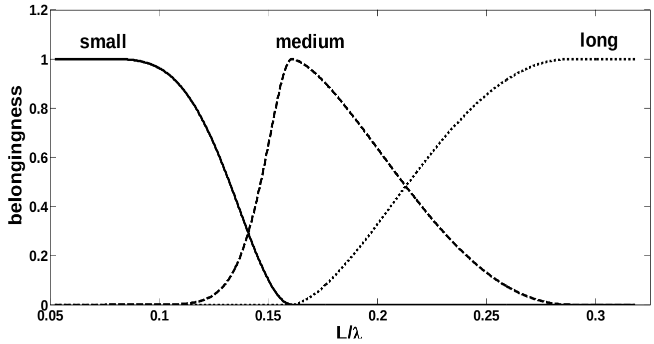

Figure 6: Membership functions for assigning three fotted lines.

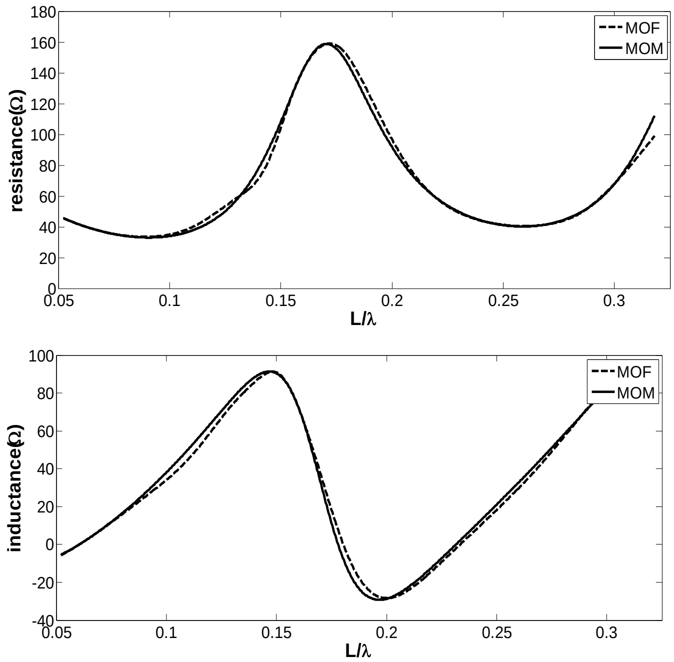

Figure 7: The predicted input impedance by MoF and MoM.

2.1 Resistivity effect of soil

In the previous sections, the resistivity of the soil was assumed to be constant, and the input impedance for arbitrary normalized length was predicted. In this section to complete the model, the effect of the resistivity of the soil is investigated. To this end, the input impedance of the soil for two values of $\rho = 800,1200(\Omega.m)$ are computed by MoM and shown in polar plane in figure 8.

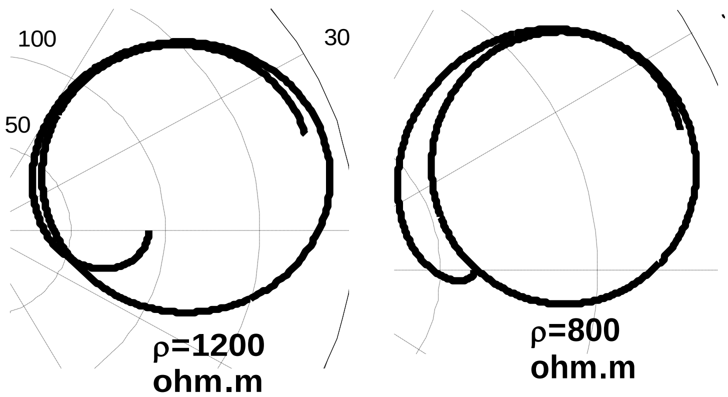

Figure 8: The input impedance in polar plane in zoomed form for two values of resistivity.

As is seen in figure 8, changing the soil resistivity is just led to changing center coordinates and radius of fitted circles. Hence, center coordinates and radius of the fitted circles for a few values of resistivity $\rho = 600,800,1000,1200,1400(\Omega.m)$ are computed by MoM and shown as stars, circles, and pluses in figure 9. Accordingly, these marks can be fitted by simple curves (of first or second order). That is, from now on center coordinates and radius for arbitrary resistivity is easily computed through these fitted curves instead of MoM. These can be considered as effect of resistivity. Figure 10 shows the predicted input impedance by the two methods, i.e., MoM and MoF for $\rho = 1000(\Omega.m)$.

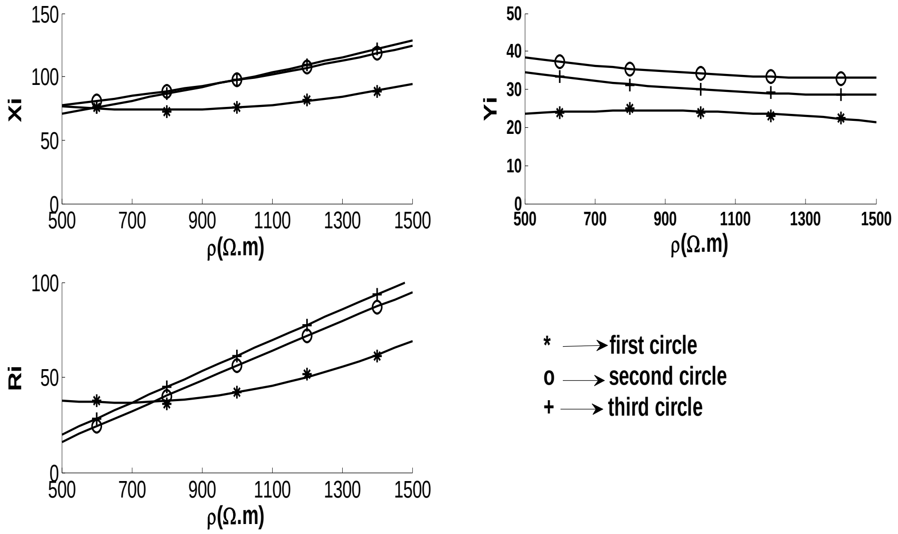

Figure 9: The effect of the resistivity on the input impedance.

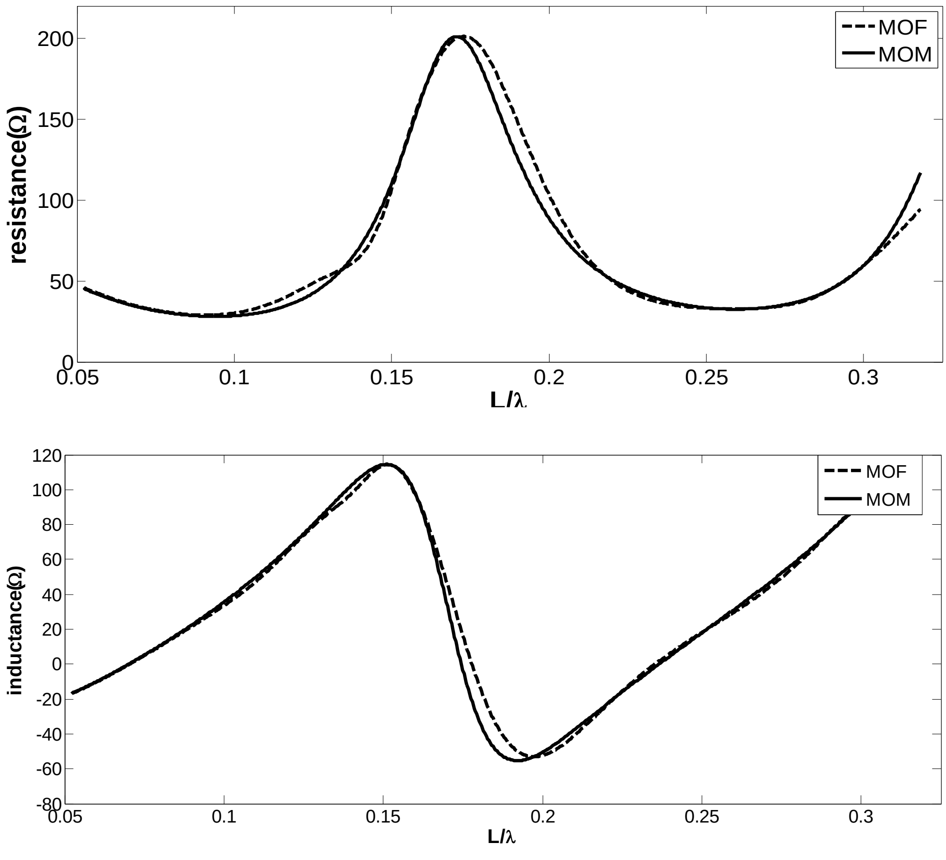

Figure 10: The predicted input impedance by MoF and MoM for $\rho = 1000\Omega.m$.

2.2 Radius effect of electrode

In the previous section, the effect of resistivity on the input impedance was obtained. In this section, similarly the effect of electrode radius is easily obtained as shown in figure 11. In the next section, in order to complete the model, these two effects are combined using spatial membership functions.

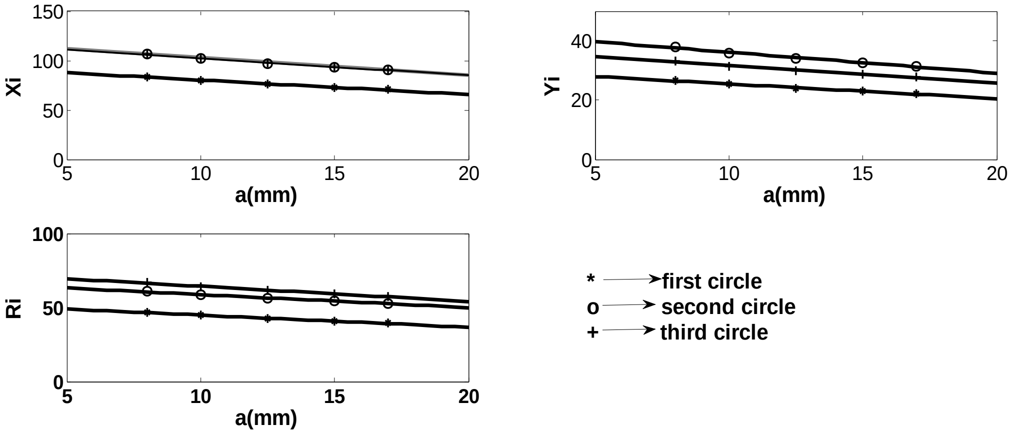

Figure 11: The effect of the electrode radius on the input impedance.

2.3 Simultaneous effects of radius and resistivity

To complete the model achieved in the previous sections, in this section the two effects extracted are combined via spatial membership functions concept. To this aim, spatial membership functions with two fuzzy sets are used as bellow:

$$\alpha_j = \begin{cases} \frac{1}{2}\left(1 - cos\left(\pi\left(\frac{\varphi-\varphi_2}{\varphi_1-\varphi_2}\right)^{\beta_1}\right)\right) & \varphi : \varphi_1 \to \varphi_2 \\ \frac{1}{2}\left(1 + cos\left(\pi\left(\frac{\varphi-\varphi_2}{\varphi_1-\varphi_2}\right)^{\beta_2}\right)\right) & \varphi : \varphi_1 \to \varphi_2 \end{cases} \tag{9}$$

Where $\varphi = tan^{-1}\left(\frac{180a}{\pi.\,\rho}\right)$, and j=a, ρ , and $(x_{i\rho}, y_{i\rho,} r_{i\rho})$ and $(x_{ia}, y_{ia,} r_{ia})$ are computed from figures 9 and 11 respectively. Also $\beta_{1,2}$ are optimizing parameters. As shown in figure 12, each fuzzy set (α_j) have belongingness one on the individual axis and is decreasing to zero on the other axis. Finally center coordinates and radius of the fitted circles representing the simultaneous effects of the resistivity and radius are inferred as equation bellow:

$$x_i\,(\rho, a) = \frac{x_{i\rho}\,.\alpha_\rho(\rho,a) + x_{ia}\,.\alpha_a(\rho,a)}{\alpha_\rho(\rho,a) + \alpha_a(\rho,a)} \tag{10}$$

$$y_i\,(\rho, a) = \frac{y_{i\rho}\,.\alpha_\rho(\rho,a) + y_{ia}\,.\alpha_a(\rho,a)}{\alpha_\rho(\rho,a) + \alpha_a(\rho,a)} \tag{11}$$

$$r_i\,(\rho, a) = \frac{r_{i\rho}\,.\alpha_\rho(\rho,a) + r_{ia}\,.\alpha_a(\rho,a)}{\alpha_\rho(\rho,a) + \alpha_a(\rho,a)} \tag{12}$$

To obtain a predefined error, $\beta_{1,2}$ are tuned using simple optimizations techniques (even by hand). The optimized spatial membership functions are shown in figure 13. As an example, the center coordinates and radius of the first fuzzy-inferred circle is shown in figure 14.

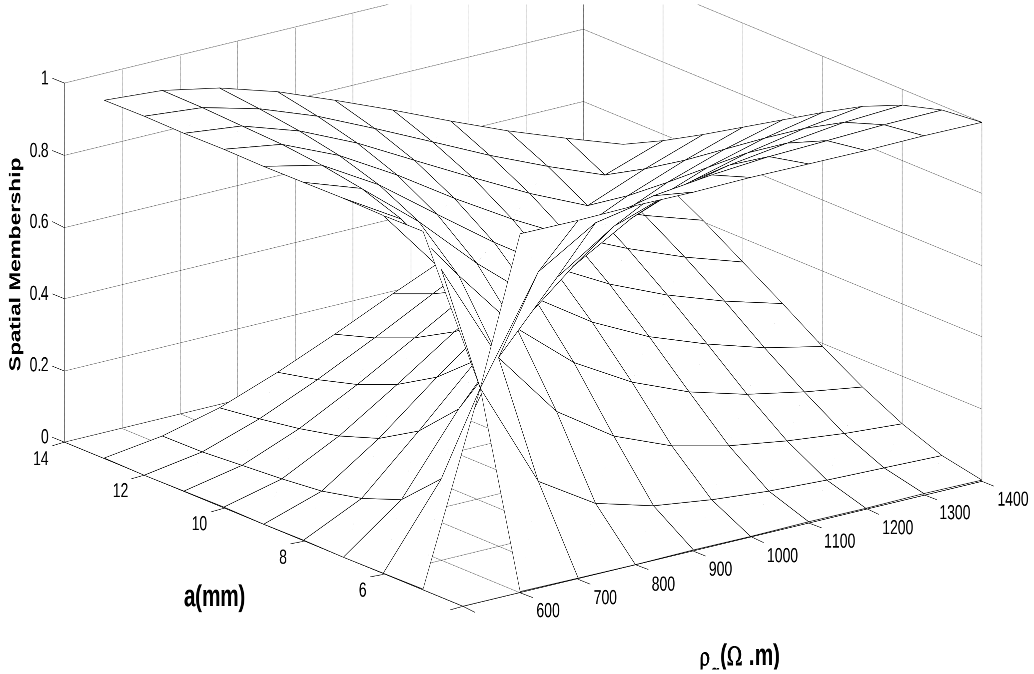

Figure 12: Spatial membership functions with two fuzzy sets for combining the effects of resistivity and radius.

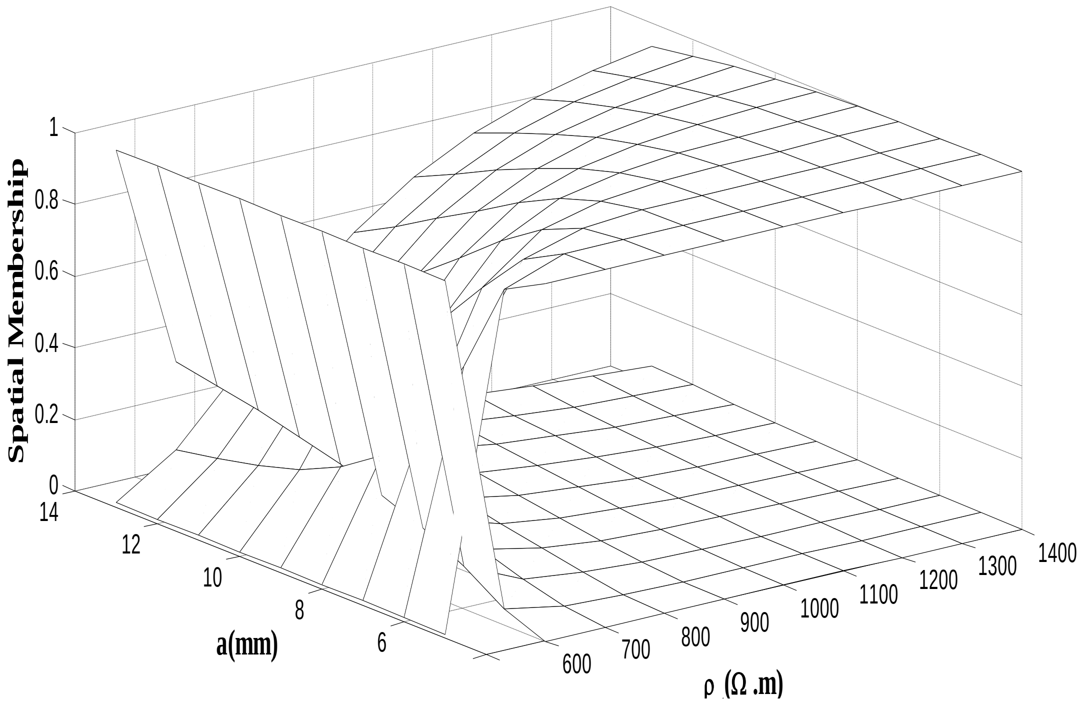

Figure 13: Optimized spatial membership functions with two fuzzy sets.

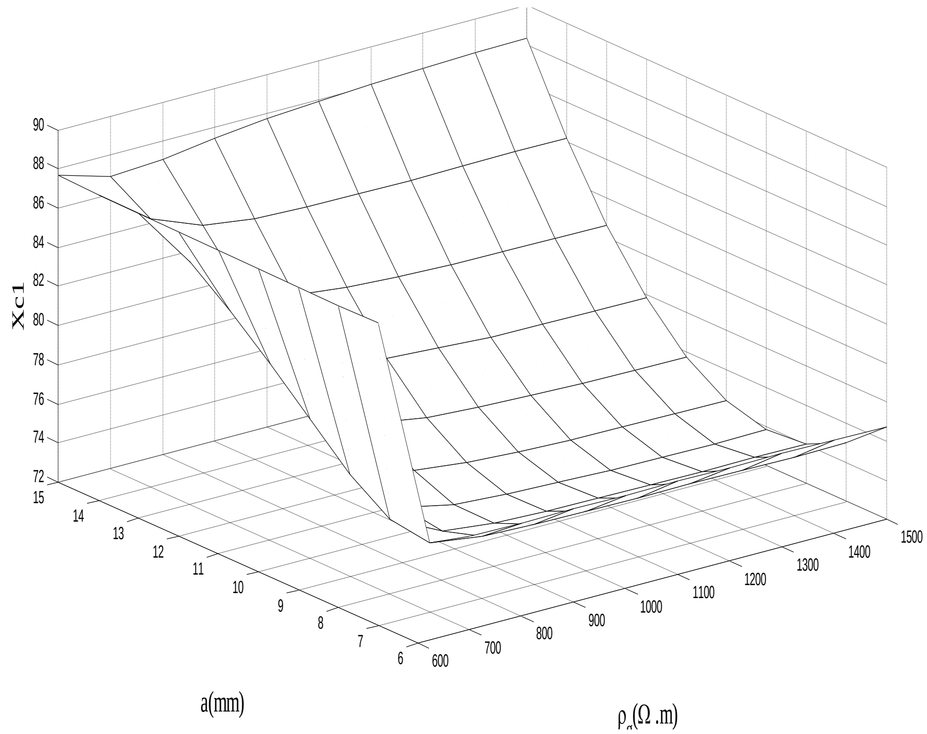
Xc1
90
88
86
84
82
80
78
76
74
72
15
14
13
12
11
10
9
8
7
6
600
700
800
900
1000
1100
1200
1300
1400
1500
a(mm)
ρs(Ω .m)

(a)

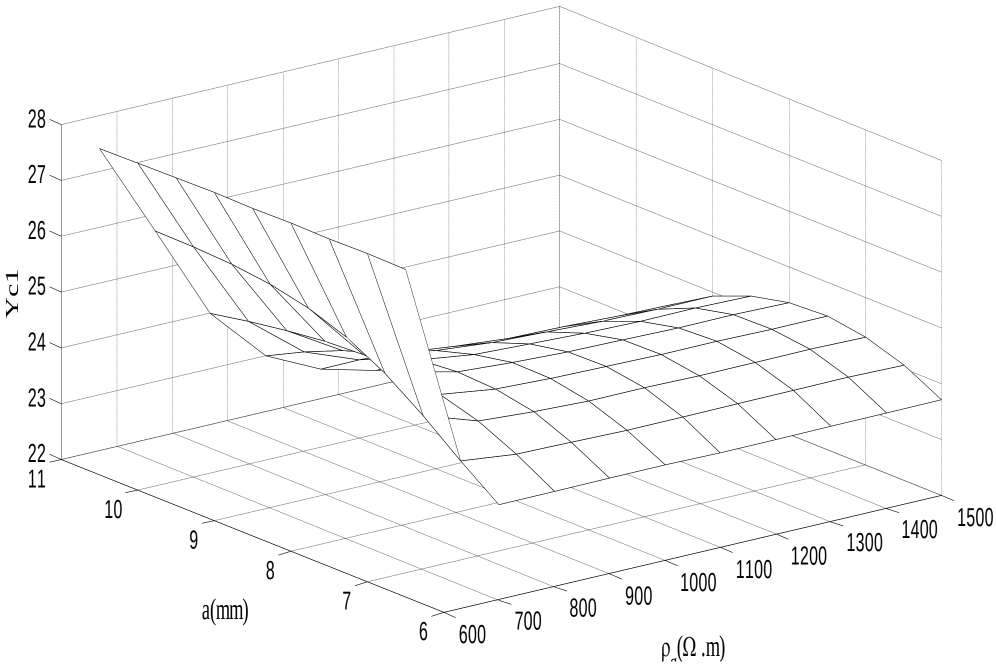
Yc1
28
27
26
25
24
23
22
11
10
9
8
7
6
600
700
800
900
1000
1100
1200
1300
1400
1500
a(mm)
ρs(Ω .m)

(b)

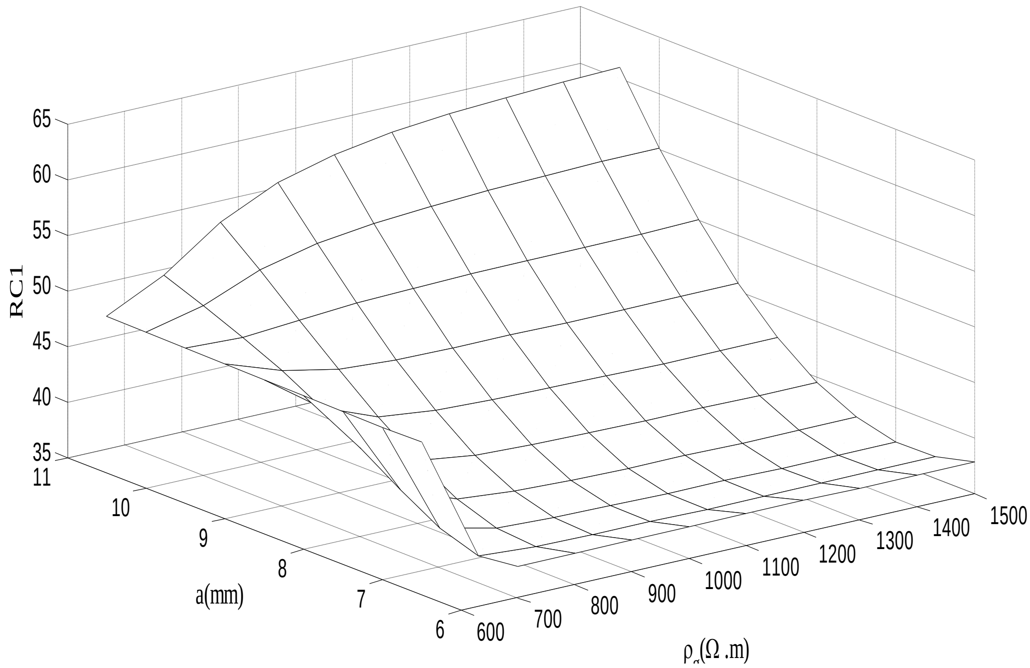

©

Figure 14: (a) and (b): center coordinates and (c): radius of the first fuzzy-inferred circle.

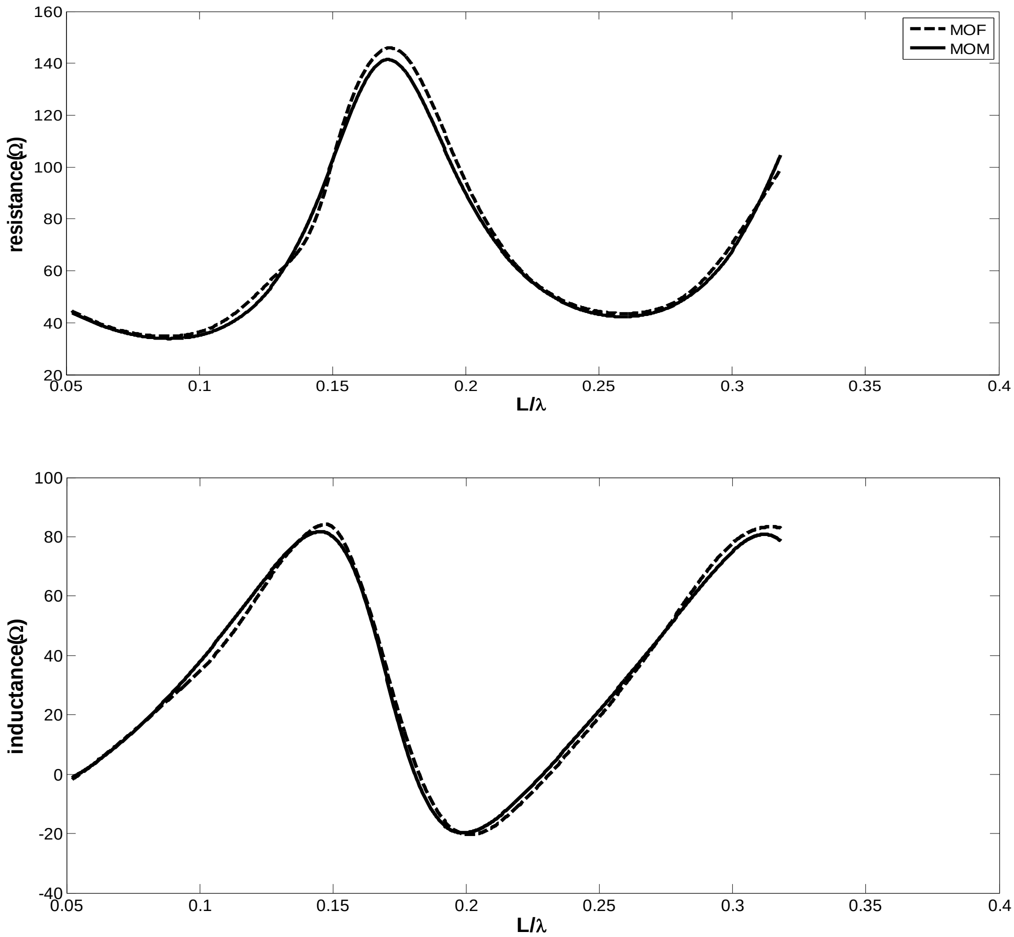

Figure 15: Predicted input impedance of the vertical electrode for $\rho = 900\Omega.m, a = 14mm$ by MoM and MoF.

3. BEHAVIOR OF HORIZONTAL ELECTRODE

In this section, consider a horizontal electrode of length $L = 10m$ and in depth $d = 1m$ inside the earth of electrical parameters $\varepsilon_r = 10$ and $\rho = 1000\Omega.m$. Since fuzzy modeling this electrode is the same as vertical one, the behavior of the electrode and the effect of resistivity are only extracted as shown in figures 16, and 17 respectively. In order to how accurate the achieved mode is, the input impedance for $\rho = 1000\Omega.m$ is computed by the two methods as shown in figure 18.

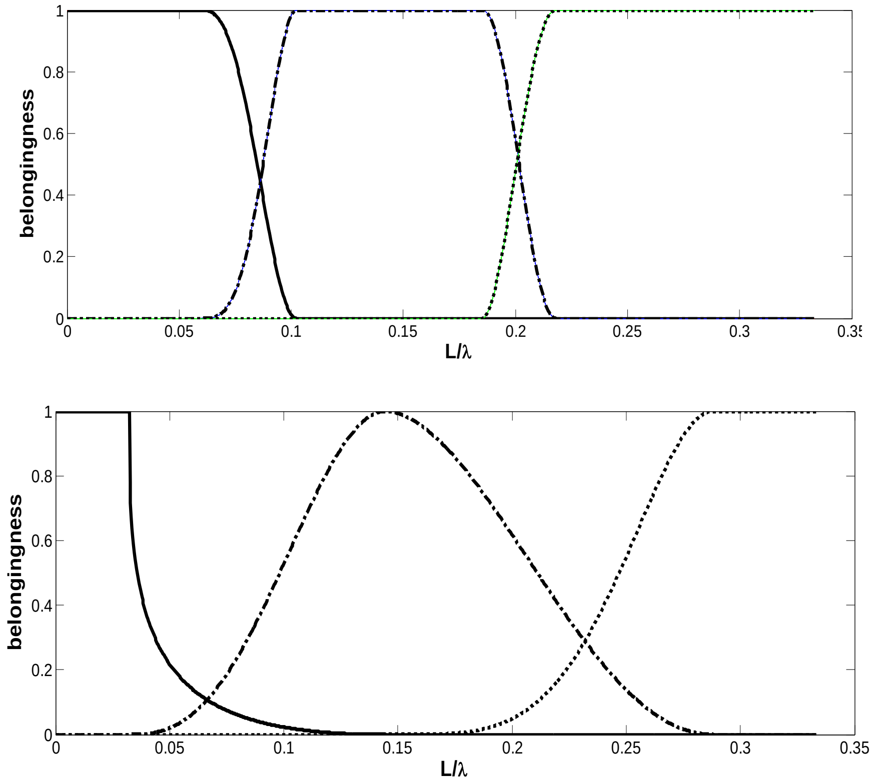

Figure 16: The membership functions for modeling (a): partial locus and (b): partial phase.

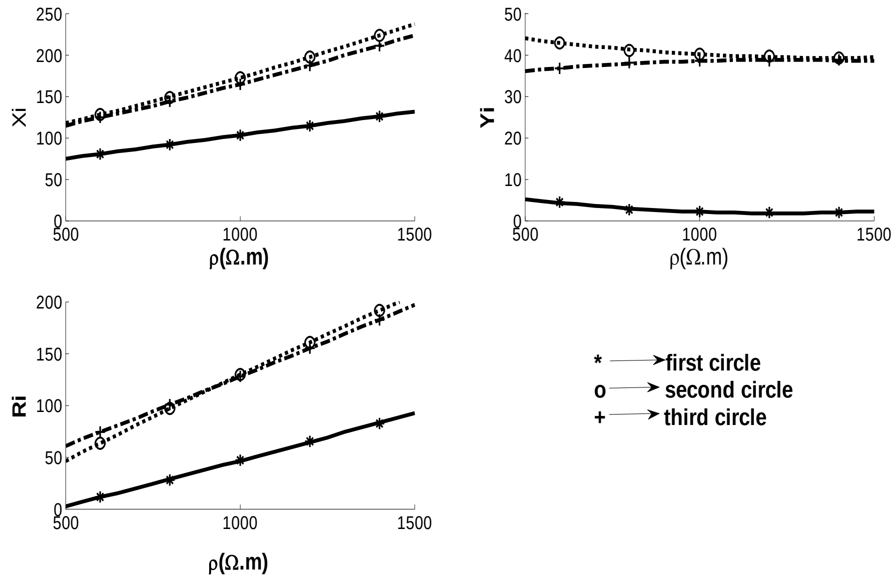

Figure 17: The effect of the soil resistivity on the input impedance of the horizontal electrode.

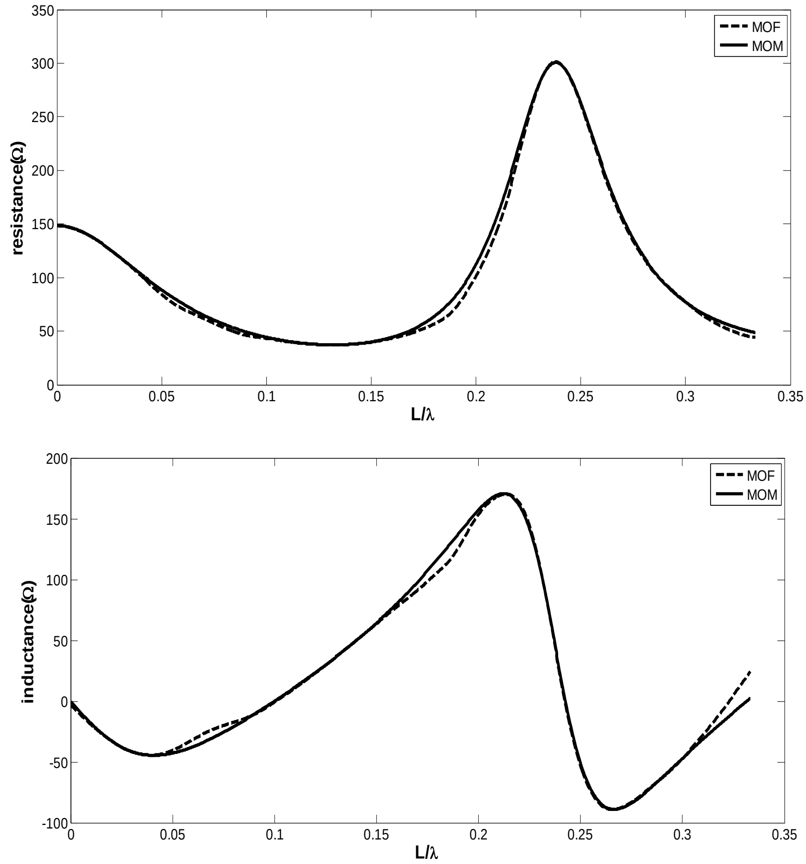

Figure 18: Predicted input impedance of the horizontal electrode for $\rho = 1000\Omega.m$ by MoM and MoF.

4. TRANSIENT VOLTAGE OF GROUNDING SYSTEMS

Once the input impedances for the two grounding systems are computed, through equation (1), transient voltage for the two surge currents is easily computed. Figure 19 and 20 shows the transient voltage for the first and subsequent strokes respectively. As it is seen in these figures, excellent agreement is achieved.

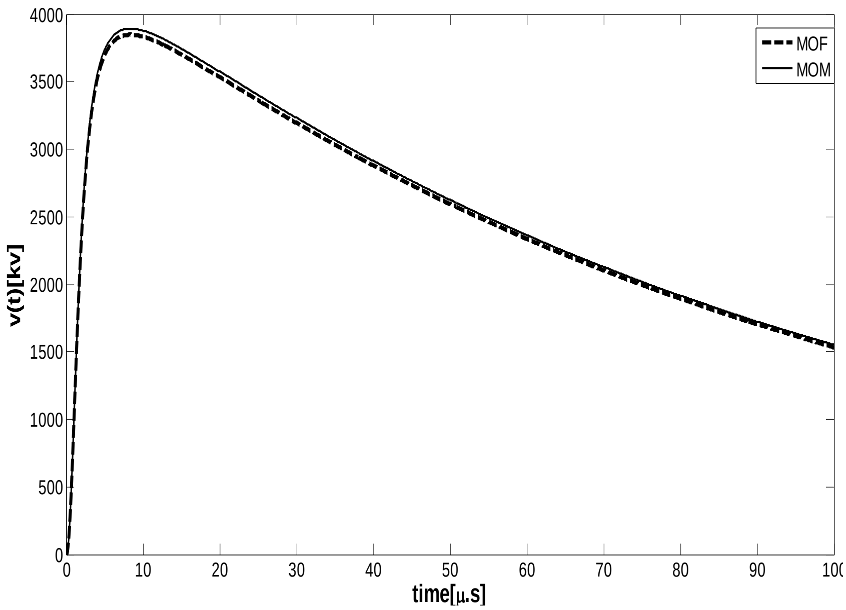

Figure 19: Transient voltage of the vertical grounding system under first stroke current.

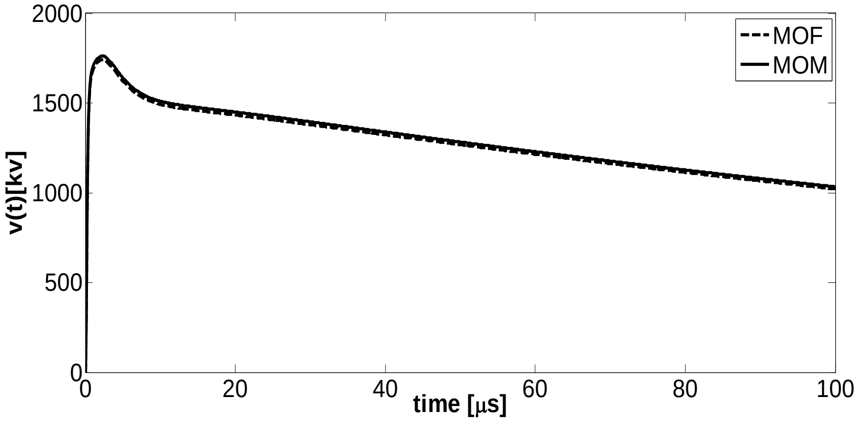

Figure 20: Transient voltage of the vertical grounding system under subsequent stroke current.

5. CONCLUSION

In this study, an efficient approach was proposed for two conventional grounding systems, i.e., vertical and horizontal electrodes. In the proposed method, at first behavior of the problem was extracted in if-then rules, and then effect of problem parameters was extracted as very simple curves. Finally through FFT and IFFT, transient voltage is efficiently computed.

6. ACKNOWLEDGEMENT

The author would like to express their sincere gratitude to Arak University its their financial supports.

7. REFERENCES

[1] Leonid Grcev, Modeling of Grounding Electrodes under Lightning Currents, *IEEE Trans. Electromagn. Compat*, vol. 51, NO. 3, Aug 2009.

[2] Thottappillil, “An Improved Transmission-Line Model of Grounding System,” *IEEE Trans. Electromagn. Compat*, vol. 43, no. 3, Aug 2001.

[3] Leonid Grcev, and Marjan Popov, “On High-Frequency Circuit Equivalents of a Vertical Ground Rod,” *IEEE Trans. Power Del*, vol. 20, NO. 2, April 2005.

[4] Majid Akbari, et al, “The Effect of Frequency Dependence of Soil Electrical Parameters on the Lightning Performance of Grounding Systems,” *IEEE Trans. On Electro Mag. Compat.*, Vol. 55, No. 4, 2013.

[5] S. Visacro, “A Comprehensive Approach to the Grounding Response to Lightning Currents,” IEEE Trans. On Power Delivery, Vol. 22, No. 1, pp. 381-386, 2007.

[6] M. I. Lorentzu, et al, “Time Domain Analysis of Grounding Electrodes impulse Response,” *IEEE Trans. Power. Del.*, Vol. 18, pp. 517-524, 2003.

[7] M. Tayarani “A novel approach to analysis and modeling of engineering electromagnetic problems and its applications by means of fuzzy interference methods based on new expressions for electromagnetic basic concepts", Ph. D thesis dissertation, University of Electro-Communications, Tokyo ,Japan, 2001.

[8] S. R Ostadzadeh, M. Tayarani, and M. Soleimani, “A hybrid model in analyzing nonlinearly loaded dipole antenna and finite antenna array in the frequency domain”, *International Journal of RF and Microwave*, vol. 19, pp. 512–518, 2009.

[9] S. R Ostadzadeh, “An Efficient hybrid model in analyzing nonlinearly loaded dipole antenna above Lossy Ground in the Frequency Domain”, Applied Computational Electromagnetic Society (ACES) Journal, vol. 28, No. 9, pp. 780–787, 2013.

[10] S. B.Shouraki, N. Honda “Fuzzy Prediction; A Method for adaption," 14th fuzzy Symposium, Gifu, Japan, 1988, pp.317-320.

[11] S. Bagheri Shouraki and N. Honda, “Fuzzy Prediction, A method for Adaptation,” 14th Fuzzy symposium, Gifu, Japan, June, 1998, pp.317-320.